

Low-temperature Ru-Sapphire Film Thermometer and Its Application in Heat Capacity Measurements

Yang-Yuan Chen

Institute of Physics, Academia Sinica, Taipei, Taiwan, 115 Republic of China

Abstract. We have measured the resistance and magnetoresistance of the recently invented Ru-sapphire film thermometers in magnetic fields up to 9 T at temperatures 0.4 K to 300 K. Compared to the present thermometers these thermometers have very small field-induced temperature deviations; in $H=9$ T the temperature deviation dT/T is $\sim 2\%$ at 2 K and $\sim 0.5\%$ at 4 K, respectively. For calorimetric applications, the film thermometer is deposited on a thin sapphire chip, and a heater is employed to measure the heat capacity of a CeCo_2 specimen of nanoparticles. Its fast response time $\tau (< 1 \text{ ms})$, small thermal mass $\sim 5 \times 10^{-7} \text{ J/K}$ (at 4 K) and high sensitivity demonstrate the potential of the integrated chip as a microcalorimeter.

INTRODUCTION

In the past decades RuO_2 resistors and RuO_2 -glass thick-film resistors [1,2] have been widely used as low-temperature thermometers. The advantage of these thermometers is their low magnetoresistance $dR(H)/R(0 \text{ T})$, typically within 2 to 3 % in a field $H=10$ T at 2 K [3]. Their logarithmic sensitivity, represented by $S = d(\log R)/d(\log T)$, is ~ 0.8 at 1 K and ~ 1.7 at 0.1 K respectively. This sensitivity is appropriate for temperatures less than 5 K; however it drops drastically for temperatures greater than 5 K. Semiconductor thermometers such as silicon and germanium are widely used cryogenic thermometers too. Unfortunately their large magnetoresistances make them useless in magnetic fields.

For cryogenic applications carbon glass is another alternative especially for the use in magnetic fields. The recently developed zirconium oxynitride film (Cernox thermometer) [4], exhibiting low magnetoresistance, has gradually become another popular thermometer in the last ten years. Nevertheless, the fabrication of a zirconium oxynitride film requires a precise control of reactive gasses in order to gain a specific composition for the desired temperature region [5].

More recently we invented a new composite Ru-sapphire film resistor. Its semiconductor-like dependence of resistance on temperature and low magnetoresistance make the film resistor an optimal cryogenic thermometer. A monotonic variation of resistance with temperature and a low magnetic-field-induced temperature error have been observed in the film resistors. These thermometers have proven to be very stable over repeated thermal cycling. In addition, the film resistor is physically hard and chemically resistant. The small thermal mass and excellent thermal conductance make it greatly suitable for applications in calorimetry.

EXPERIMENTS AND RESULTS

RuO_2 Film Thermometers

The composite Ru-sapphire film resistors, consisting of RuO_2 and Al_2O_3 , are fabricated on sapphire single crystals (Al_2O_3). The material and structural similarity between the film resistor and the substrate is a significant factor in growing high quality films and film-substrate bonds. The natural integration of the films with the substrate gives the thermometer and substrate, as a whole assembly, an excellent

thermal conductance. By varying the relative composition of components, film resistors can be fabricated with a desired temperature coefficient of resistance $TCR = (1/R) (dR/dT)$.

The resistances of four thermometers having different compositions have been measured by the standard four-probe method, and the results are shown in Fig.1. From left to right the weight percentage of RuO_2 is reduced from roughly $\sim 80\%$ to $\sim 40\%$. Although the exact compositions are not available quantitatively, it shows that the thermometer with a smaller fraction of RuO_2 exhibits a larger TCR and room-temperature resistance. This result is consistent with other types of film resistors composed of conducting and insulating components [6].

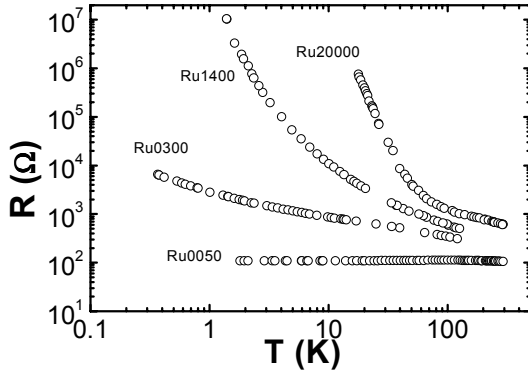


FIGURE 1. Temperature-dependent resistances for four Ru-sapphire thermometers having different compositions. The indices represent the lowest temperature (in millikelvins) of the thermometer that can possibly be measured.

To further study their physical properties in magnetic fields, the temperature dependence of resistance for another Ru1400 thermometer was measured, as shown in Fig. 2. The room-temperature resistance, $\sim 2\ \Omega$, which is much smaller than the one shown in Fig. 1, is due to the additional deposition of Au electrodes; the details will be explained later. The resistance increases monotonically as temperature decreases with a resistivity ratio $R(4.2\ K)/R(300\ K) \sim 150$. Its sensitivity dR/dT is $\sim 10^5\ \Omega/K$ at 4.2 K and $\sim 10^2\ \Omega/K$ at 30 K respectively. To be a practical low-temperature thermometer, high temperature sensitivity is required. Our thermometers indeed satisfy the criterion.

The inset to Fig. 2 shows its logarithmic sensitivity $d(\log R)/d(\log T)$. A relatively sharp

transition near the critical temperature $T_c \approx 20\ K$ is noticed; below T_c the sensitivity increases significantly with a decrease in temperature. Its logarithmic sensitivity $S \approx -3.5$ at 2 K and $S \approx 0.8$ at 100 K are quite competitive with other available sensors.

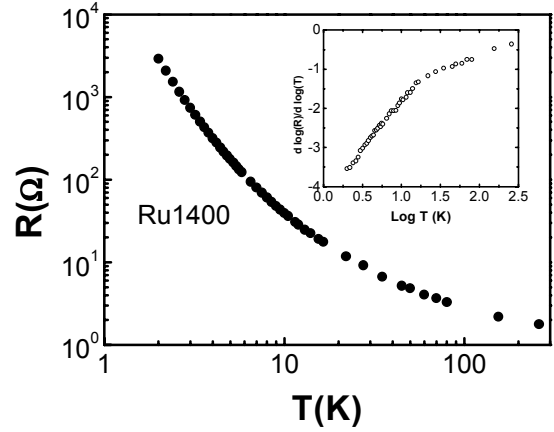


FIGURE 2. Temperature dependence of resistance for a Ru 1400 thermometer. Inset: temperature dependence of logarithmic sensitivity $d(\log R)/d(\log T)$.

Magnetoresistance

The magnetoresistance of the thermometer measured at selected temperatures in magnetic fields up to 9 Tesla is shown in Fig. 3. At low fields the magnetoresistance $\Delta R(H) = [R(H) - R(0\ T)]$ is positive, becoming negative as the magnetic field increases above a turning point H_c . For instance at 2 K, the magnetoresistance slowly increases to a positive maximum 3.2% at $H = 1.8\ T$ as the magnetic field initially increases. After that it goes through zero at a critical field $H_c = 3.5\ T$ before decreasing to a negative value -7% at 9 T.

For higher measuring temperatures, a similar field dependence of magnetoresistance is observed, except with a smaller magnitude. The critical field H_c also shifts to a larger value at higher temperatures, for example H_c increases from 3.5 T to 7 T as temperature increases from 2 K to 5 K. In the inset to Fig. 3, we plot the magnetoresistance versus measuring temperature in $H = 9\ T$. The magnetoresistance gradually decreases to a negligible magnitude as temperature approaches to 6 K.

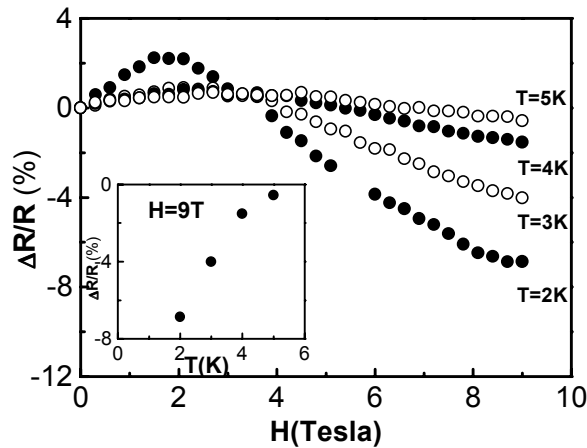


FIGURE 3. Magnetoresistance of Ru1400 versus magnetic field at selected temperatures, where $\Delta R(H)/R(0\text{ T}) = (100\%) [R(H) - R(0\text{ T})]/R(0\text{ T})$. Inset: temperature dependence of magnetoresistance at $H = 9\text{ T}$.

The corresponding field-induced temperature error due to magnetoresistance, defined as $\Delta T(H) / T(0\text{ T}) = [T(H) - T(0\text{ T})] / T(0\text{ T})$ can be derived from $\Delta R/R$ and $d(\log R)/d(\log T)$ according to the formula $\Delta T(H)/T(0\text{ T}) = [\Delta R/R]/[d(\log R)/d(\log T)]$. The results are shown in Fig. 4.

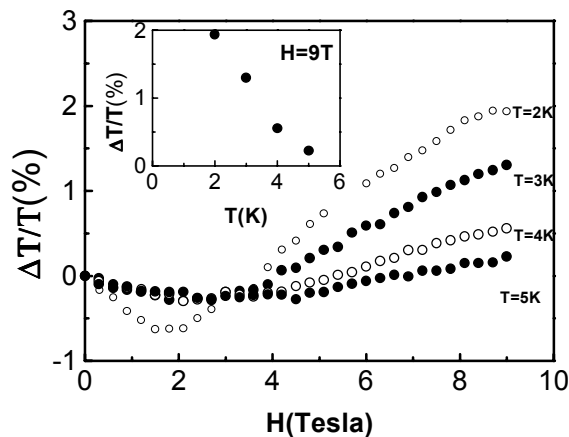


FIGURE 4. Temperature deviation of Ru1400 versus magnetic field at selected measuring temperatures. $\Delta T(H)/T(0\text{ T}) = (100\%) [T(H) - T(0\text{ T})] / T(0\text{ T})$. Inset: temperature dependence of temperature deviation at $H = 9\text{ T}$.

The magnetic-field-induced temperature deviation increases as the temperature decreases; 2 % is the maximum found at 2 K and 9 T. Basically this is analogous to the field dependence of $\Delta R(H)/R(0)$ in Fig. 3 with changes in magnitude and sign. In the

inset to Fig. 4, we plot the temperature deviation versus measured temperature for $H = 9\text{ T}$. The temperature deviation asymptotically falls to an insignificant magnitude as temperature approaches to 6 K.

It has been reported that the magnetoresistance of composite materials is independent of the relative directions of applied field and measuring current [4]. We have performed similar measurements on some thermometers by changing the orientation of the field to the measuring current and to the film's plane. As before, no noticeable change in magnetoresistance can be found.

Microcalorimeter

Taking advantage of the excellent thermal conductance and small thermal mass of the integrated Ru-sapphire film and substrate, a microcalorimeter was fabricated for heat capacity measurements. A thin sapphire chip with dimensions of $2.95 \times 2.95 \times 0.2\text{ (mm)}^3$ is used as a sample holder on which a Ru-sapphire film resistor and a heater are deposited (as shown in Fig. 5) [6].

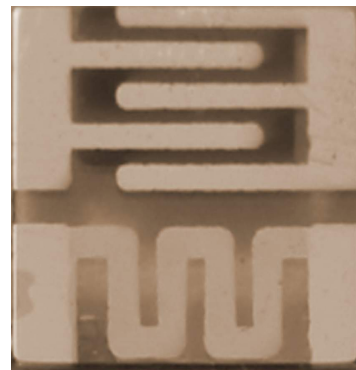


FIGURE 5. Microcalorimeter: a square sapphire single crystal on which a Ru-sapphire film thermometer (middle part of the top half) and a Ni-Cr heater (bottom half) are deposited. Four Au pads at the corners are used for electrical wire bonding.

The heater, a serpentine Ni-Cr film having a temperature independent resistance $\sim 2000\ \Omega$, is used to deliver a heat pulse to the specimen. The thermometer is employed to record the temperature of the holder and the sample. The resistance of the bare film resistor is in the range of a few kilohms. To reduce the resistance of the film to a suitable

magnitude for easy measurement, a comb shape of Au electrodes is deposited on the film resistor. Four wires of 8 %Au–Cu alloy with a length ~ 6 mm were bonded to the corners of the square for mechanical support, electrical connections and thermal links to a heat sink. The measurements of heat capacity were performed using the thermal-relaxation technique in a ^3He refrigerator from $T = 0.5$ K to 50 K [7, 8]. The heat capacity is calculated according to the formula $C = K\tau$, where K is the thermal conductance of thermal links and τ is the temperature relaxation time constant recorded from the temperature relaxation curve.

The heat capacity of the empty holder (microcalorimeter) is measured first for the purpose of background subtraction in later specimen measurements. For $T < 1.2$ K the measured τ is much less than the time resolution ~ 5 ms of our data acquisition electronics; thus only the valid data for $T \geq 1.2$ K is plotted (Fig. 6).

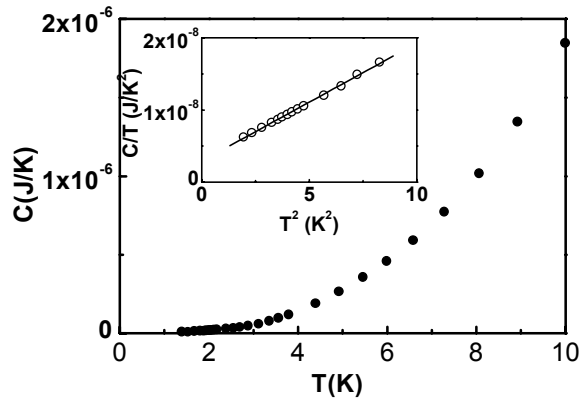


FIGURE 6. Temperature dependence of heat capacity of an empty sample holder SP0300. Inset: the heat capacity is well fit to the equation $C/T = \gamma + \beta T^2$.

The heat capacity of the holder, consisting of the contributions from conduction electrons γT and lattice phonons βT^3 , can then be represented by and fit to the equation $C = \gamma T + \beta T^3$. The temperature dependence of heat capacity is plotted as C/T versus T^2 in the inset to Fig. 5 with fitting parameters of $\gamma = 3 \times 10^{-9}$ J/K² and $\beta = 1.7 \times 10^{-9}$ J/K⁴. At 4 K the heat capacity of the sapphire square is about 5×10^{-7} J / K, which is approximately equivalent to a 1 μm thickness CeCo_2 film with mass ~ 100 μg . Owing to such a small background of the calorimeter, the specific heat of specimens like nanoparticles or films can be measured most opportunely.

To estimate the response time of the calorimeter, defined as the time needed for the calorimeter itself to reach thermal equilibrium, the observation of the τ_2 effect would be an adequate method. The scenario is that if the response time is longer than the measuring time, then an additional thermal relaxation time τ_2 besides the primary one (τ) will be observed [9]. Indeed no τ_2 effect could be detected in the above measurements. Based on the electronic resolution of 5 ms, the response time is estimated to be less than 1 ms.

To demonstrate the capability of the microcalorimeter to measure samples of small mass such as nanoparticles, a specimen of CeCo_2 nanoparticles with mass ~ 0.4 mg was attached to the microcalorimeter using N-grease and its heat capacity was measured. After subtracting the backgrounds of the microcalorimeter and grease, the net heat capacity of the specimen was obtained. The molar heat capacity of the specimen was calculated and plotted in Fig. 7. A low-temperature anomaly below 2 K is slightly revealed. After phonon subtraction it becomes clear and is identified as the contribution of Kondo interactions by data analysis.

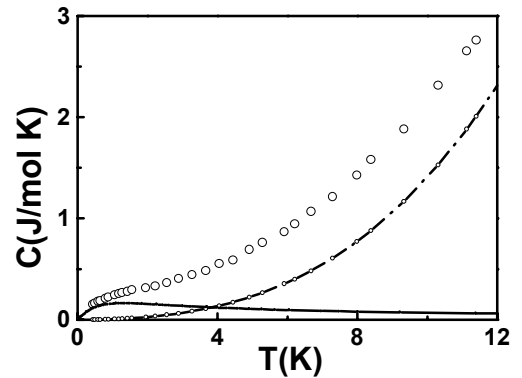


FIGURE 7. Temperature dependence of the heat capacity of CeCo_2 nanoparticles (open circles). The dotted line represents the heat capacity of the phonon contribution; the solid line represents the Kondo contribution.

In conclusion, a newly invented Ru-sapphire film resistor, having small a field-induced temperature error of $\sim 2\%$ at $T = 2$ K and $H = 9$ T, is demonstrated to be an excellent cryogenic thermometer. A microcalorimeter made of this thermometer reveals its advantages in the aspects of thermal mass and response time. It is potentially suitable for studying small specimens such as nanoparticles or films.

REFERENCES

1. Zhang, B., Brooks, J. S., Perenboom, J. A. A. J., Han, S.-Y., and Qualls, J. S., *Rev. Sci. Instrum.* **70**, 2026 (1999).
2. Bat'ko, I., Flachbart, K., Somora, M., and Vanicky, D., *Cryogenics* **35**, 105 (1995).
3. Li, O., Watson, C. H., Goodrich, R. G., Haase, D. G., and Lukefahr, H., *Cryogenics* **26**, 467 (1986).
4. Brandt, B. L., Liu, D. W., and Rubin, L. G., *Rev. Sci. Instrum.* **70**, 104 (1999).
5. Swinehart et al. USA patent number 5367285 (1994).
6. SP0300 of MAS Top Industrial Corp. 526 S. Coral Ridge Pl., City of Industry, CA 91746, USA.
7. Schwall, R. E., Howard, R. E., and Stewart, G. R., *Rev. Sci. Instrum.* **46**, 1054 (1975).
8. Chen, Y. Y., Yao, Y. D., Hsiao, S. S., Jen, S. U., Lin, B. T., Lin, H. M., and Tung, C. Y., *Phys. Rev. B* **52**, 9364 (1995).
9. Sullivan, Paul F., and Seidel, G., *Phys. Rev.* **173**, 679 (1968).